Contemporary Mathematics
http://ojs.wiserpub.com/index.php/CM/

Research Article

Applications of the Nonstandard Finite Difference Method to a Fractional Model Explaining Diabetes Mellitus and Its Complications

Said Al Kathiri[1*], Farah Aini Abdullah[1], Nur Nadiah Abd Hamid[2], Eihab Bashier[3], Altaf A Bhat[4], Danish A Sunny[4]

[1] School of Mathematical Sciences, Universiti Sains Malaysia, 11800, USM, Pulau Penang, Malaysia
[2] Nur Nadiah Academic Services, Butterworth, Pulau Pinang, Malaysia
[3] Faculty of Education and Arts, Sohar University, Sohar, Oman
[4] Mathematics and Computing Skills Unit, Preparatory Studies Center, University of Technology and Applied Sciences, Salalah, Sultanate of Oman
E-mail: said2021@student.usm.my

Received: 10 September 2024; **Revised:** 28 October 2024; **Accepted:** 11 November 2024

Abstract: This work examines a mathematical model of high blood sugar conditions and its consequences in a society using fractional differential equations. It attempts to solve the problem using a nonstandard way because standard finite difference numerical methods can result in numerical instabilities. The nonstandard finite difference scheme (NSFDS), which satisfies dynamical consistency, is the recommended nonstandard method for discretising the model. To show that the model is stable at the equilibrium positions, analyses of both discrete and continuous models are studied.Stability analysis is carried out at the discretised model's equilibrium point using the Schur-Cohn criterion. Consequently, the model's asymptotically stable state is demonstrated. Furthermore, by contrasting the stability for various step sizes with conventional techniques like Finite Difference Scheme (FDS), the benefits of the NSFDS are shown. The NSFDS has been shown to converge at bigger step sizes. Furthermore, a graphical comparison is shown between the numerical findings acquired by the NSFDS and the FDS. It is noted that the NSFDS is accurate.

Keywords: diabetes mellitus, nonstandard finite difference scheme, stability analysis, fractional calculus

MSC: 34A30, 65L07

Abbreviation

NSFDS	Nonstandard finite difference scheme
FDS	Finite difference scheme

1. Introduction

Differential equations can be applied to model a diversity of biological issues. As is well known, diabetes has recently become a highly prevalent condition. Numerous significant studies on diabetes have been conducted. Stability analysis

Copyright ©2024 Said Al Kathiri, et al.
DOI: https://doi.org/10.37256/cm.5420245701
This is an open-access article distributed under a CC BY license
(Creative Commons Attribution 4.0 International License)
https://creativecommons.org/licenses/by/4.0/

plays a crucial part in epidemic models. The following is a summary of some diabetes research: In order to provide a higher quality for people, the authors in [1] suggest a mathematical model of high blood sugar. They provided the linear model's numerical solution and stability analysis, where the unknowns are the proportion of diabetics with and without issues. In their research, Akinsola and Oluyo [2–4] used various techniques to arrive at the numerical and analytical solution of the diabetes mellitus complications and control model. Furthermore, AlShurbaji et al. [5] consider the linear diabetes mellitus model. Numerical techniques including Euler, Heun, Runge-Kutta, and Adams-Moulton were applied to get the solution of a system of linear differential equations. Additionally, the Euler-Cauchy approach was used to offer a numerical solution by Vanitha and Porchelvi [6]. By using the right parameters, the authors in [7] constructed a nonlinear mathematical model of high blood sugar conditions. Numerical experiments and stability analysis are presented. Global asymptotic stability and the model suggested in [7] were taken into consideration by De Oliveira et al. [8]. Numerical simulations were used to confirm stability. The dynamics of a population of healthy individuals, diabetics and pre-diabetics with and without problems were given by authors in [9]. The theory of best favorable is applied. Controllability and stability for both linear and nonlinear differential equations were demonstrated by Permatasari et al. [10], who worked on the model created in [9]. The nonlinear diabetic mellitus model was examined by Widyaningsih et al. [11] in relation to genetic and lifestyle factors. The number of deaths from diabetes was predicted using the 4th-order Runge-Kutta method. A model that is linear which describes diabetes mellitus and its consequences was the subject of stability investigated by Aye [12]. The Bellman and Coke theorem was used to test the stability.Aye et al. [13] used the Homotopy Perturbation Method to solve a comparable scenario. Aye [14] investigated how to control affected the same model.

It is well known that the fields of applied mathematics heavily rely on stability analysis of mathematical models. In stability analysis, discretizing the models is crucial in real-world scenarios. Numerical instabilities might also result from using typical numerical methods to solve such situations. Nonstandard approaches are therefore important. The nonstandard finite difference scheme (NSFDS), created by Mickens [15–20], is one of the most practical and efficient discrete approaches. Additionally, it offers convergence outcomes at even larger step sizes. The studies of Patidar [21, 22] give a thorough literature review on NSFDS. Numerous applied mathematics disciplines have produced numerous studies on NSFDS. The following is a list of some recent research on NSFDS and stability analysis: A mathematical model based on the Tacoma Narrows Bridge collapse is examined by Adekanye and Washington [23]. For the torsional and vertical variants, two NSFDS are built. Anguelov et al. [24] proposed the applicability of NSFDS to Ebola virus system of model in Africa. Arenas et al. [25] introduced fractional model of epidemic for susceptible-infected-recovered (SIR) and susceptible infected (SI). There are some similarities with classical approaches after applying NSFDS. For integer and fractional order, a unique chaotic model was analyzed by Baleanu et al. [26]. In both cases stability analysis was presented. NSFDS is utilized to present numerical simulations. NSFDS are constructed for two metapopulation models by Dang and Hoang [27]. Other features including positivity, boundedness, and monotone convergence were provided along with stability analysis. The theoretical investigation was supported by numerical computations. Kocabıyık et al. [28] and Dang and Hoang [29] used the NSFDS to approximate a computer virus model. Using NSFDS, the authors in [30] build a mathematical system that describes the Michaelis-Menten harvesting rate. Kocabiyik and Ongun [31] described the NSFDS of smoking model in discretization way to ascertain the impacts on humans who smoke. In the study by Ongun and Arslan [32], two distinct NSFDS for the fractional order Hantavirus model were compared. Shabbir et al. [33] used NSFDS to build a predator-prey model. Investigations are conducted into stability analysis as well as other characteristics including positivity, boundedness, and persistence of solutions. An NSFDS for the SICA-AIDS model was put forth by Vaz and Torres [34]. Both global and elementary stability were examined. In [35], Egbelowo et al. examined a linear mathematical model of pharmacokinetics. The analytical solution, NSFDS, and Finite Difference Scheme (FDS) were shown. [36–40, 40, 41] give more recent research on the stability study of the mathematical models. Said et al. [42] presented a NSFDS for solving a fractional decay model. The proposed NSFDM was constructed by incorporating a non-standard denominator function, resulting in an explicit numerical scheme as easy as the conventional Euler method, but it provides very accurate solutions and has unconditional stability. It was found that the method's estimated errors are extremely minimal, such as within the machine precision. Iikem Cetinkaya [43] presented and described the complications of diabetes mellitus and its consequences, concluded that the model is asymptotically stable.

Extension of ordinary calculus to fractional calculus takes us into a new mathematical domain for solution of diverse problems in various fields of study, such as computational biology, probability, control theory etc. Differential equations can represent these phenomena in a better way. The properties of well-known fractional calculus were used to get solutions of certain fractional calculus equations representing these types of phenomena. The solution of most of these differ-integral equations take the form of Mittag-Leffler function, Fox-Wright functions etc. There are numerous authors who define fractional calculus. The Riemann-Liouvellie (R-L) definition is the one that is most frequently employed [44–48]. The Caputo definition of fractional derivative (1967) [44–48] is another helpful formulation. To prevent nonzero fractional derivative of a constant function, applying left hand Jumarie's version of the R-L fractional derivative is helpful [49, 50]. A theory of characterizing the points where the function is non-differentiable, using a Jumarie type right hand fractional derivative version of the R-L was recently developed by Ghosh et al. in the publication [51]. Different types of solutions were provided by differential equations in various fractional derivative forms [44–48]. Therefore, fractional differential equations cannot be solved using a normal algorithm. Therefore, a growing area of applied mathematics in fractional calculus gives the solution and interpretation of such models. Recently, the Predictor-Corrector approach [52], Adomain decomposition method [45, 53, 54], Disordered Perturbation method [55], Iteration method through variation [56], Method through differential transform [57] were employed to get the solution of both linear and non-linear differential equations. An analytical approach for solving linear FDE's with the derivatives by Jumarie [50] using sine, cosine and Mittag-Leffler functions was recently devised by Ghosh et al. [58]. The numerical analysis of the nuclear decay model and fractional population growth was presented by Alzaid et al. [59]. By applying exponential decay kernel, Alqhtani et al. [60] provided solutions of space-fractional diffusion equations numerically.

NSFDS have a particular advantage over traditional finite difference schemes because they may provide exact numerical schemes that lead to exact solutions at the nodal points. For the purpose of solving certain classes of first-order differential equations, such as the logistic and exponential growth, systems of linear ODE models, higher order ODEs, some PDE problems, etc., Micken was the first to design and explain the derivation of exact finite difference techniques [61, 62]. Initially, NSFDS were designed to offer either an accurate finite difference scheme or the optimal numerical scheme, with the goal of achieving all the solutions qualitatively of the original problem.

The purpose of this piece of work is to design a numerical scheme employing nonstandard finite difference discretization to solve the diabetes model and its consequences given in linear fractional differential equations. It compares the performance of the proposed scheme to other methods found in the literature. The main features of the proposed numerical approach are its explicit Euler method-like design, high order of convergence, and unconditional stability.

The paper is organized in the following manner:

Section 1 provides an insight of fractional calculus and the development of an NSFDS. The mathematical preliminaries are given in section 2. In the Section 3 proposed methodology is introduced. Section 4 employs numerical examples from existing literature to evaluate the validity of the proposed technique. Finally, the discussion and conclusions are presented in Section 5.

2. Mathematical preliminaries

Definition 2.1 Riemann-Liouville (R-L) fractional derivative:

The fractional Riemann-Liouville (R-L) left derivative is given by,

$$ {}_bD_z^{\alpha} f(z) = \frac{1}{\Gamma(n+1-\alpha)} \left(\frac{d}{dz}\right)^{n+1} \int_b^z (z-\tau)^{n-\alpha} f(\tau) d\tau, \tag{1} $$

where $n \leq \alpha < n+1$, n is positive integer.

When $0 \leq \alpha < 1$ then

$$ {}_bD_z^{\alpha} f(z) = \frac{1}{\Gamma(1-\alpha)} \frac{d}{dz} \int_b^z (z-\tau)^{-\alpha} f(\tau) d\tau. \tag{2} $$

The corresponding fractional Riemann-Liouville (R-L) right derivative is given as follows:

$$ {}_zD_b^{\alpha} f(z) = \frac{1}{\Gamma(1-\alpha)} \frac{-d}{dz} \int_z^b (\tau-z)^{m-\alpha} f(\tau) d\tau, \tag{3} $$

where $n \leq \alpha < n+1$.

According to the definitions (1)-(3) above, a constant's derivative is non-zero, which is in opposition to the constant's classical derivative of zero. A revision to the R-L concept of fractional derivative was offered by Caputo [29] in 1967 in order to get around this drawback.

Definition 2.2 Caputo Derivative:

Fractional derivative defined by Caputo is given in the following form [49]:

$$ {}_b^C D_z^{\alpha} f(z) = \frac{1}{\Gamma(m-\alpha)} \int_b^z (z-\tau)^{m-\alpha-1} f^m(\tau) d\tau, \tag{4} $$

where $m-1 \leq \alpha < m$.

In this concept, $f(x)$ is differentiated n times first, and then $n-\alpha$ times are integrated. This method's drawback is that $f(x)$ needs to be n times differentiable for the existence of α-th order, where $m-1 \leq \alpha < m$. This definition is not applicable if the function is non-differentiable. This method has two key advantages:

(i) the derivative of a constant is zero in fractional way; and

(ii) the initial conditions of the R-L type differential equations are fractional type, whereas the Caputo type fractional differential equations have classical derivative type initial conditions.

This indicates that a fractional differential equation including R-L fractional derivatives necessitates an understanding of fractional initial conditions, which can occasionally be challenging to physically interpret [45].

Definition 2.3 Jumaire type fractional derivative:

In order to get around the fractional derivative of a constant that is not zero, Jumarie [50] suggested another way to define the left R-L type fractional derivative in the interval $[a,\ b]$ of the function $f(x)$ in the form as follows:

$$ f_L^{(\alpha)}(z) = {}_a^J D_z^{\alpha} f(z) \tag{5} $$

$$ = \begin{cases} \dfrac{1}{\Gamma(-\alpha)} \displaystyle\int_a^z (z-\tau)^{-\alpha-1} f(\tau) d\tau, \ \ \alpha < 0 \\ \dfrac{1}{\Gamma(1-\alpha)} \dfrac{d}{dz} \displaystyle\int_a^z (z-\tau)^{-\alpha} (f(\tau)-f(a)) d\tau, \ \ 0 < \alpha < 1 \\ \left(f^{(\alpha-n)}(z) \right)^{(n)}, \ \ n \leq \alpha < n+1. \end{cases} $$

For $z < a$, they assume that $f(z) - f(a) = 0$. The R-L derivative of order α $(0 < \alpha < 1)$ of the offset function $(f(x) - f(a))$ is shown in the second line of equation (5), while the first expression represents fractional integration. They employ the third line for $\alpha > 1$, which means that they apply complete n order differentiation to the offset function with order $0 < (\alpha - n) < 1$ after first differentiating it using the formula of the second line. In this case, they selected the integer n, which is just less than the real number α $(n \leq \alpha < n+1)$.

Definition 2.4 Mittag-Leffler function:

This function was defined and explored by Mittag-Leffler. The exponential function, e^x, is directly generalized by this function, which is an essential part of fractional calculus. Power series expansion has been used to define the one, two, and three-parameter Mittag-Leffler functions as follows [63–65].

$$E_{\alpha}(x) = \sum_{i=0}^{\infty} \frac{x^i}{\Gamma(1+\alpha i)}, \quad \text{for} \quad \alpha \in C,\ Re(\alpha) > 0. \tag{6}$$

$$E_{\alpha,\,\beta}(x) = \sum_{i=0}^{\infty} \frac{x^i}{\Gamma(\beta+\alpha i)}, \quad \text{for} \quad \alpha,\ \beta \in C,\ Re(\alpha) > 0. \tag{7}$$

$$E^{\gamma}_{\alpha,\,\beta}(x) = \sum_{i=0}^{\infty} \frac{(\gamma)_i x^i}{\Gamma(\beta+\alpha i) i!}, \quad \text{for} \quad \alpha,\ \beta,\ \gamma \in C,\ Re(\alpha) > 0. \tag{8}$$

where, $(\gamma)_i = \gamma(\gamma+1)(\gamma+2)(\gamma+3)...(\gamma+i-1)$ and $(\gamma)_0 = 1$.

The representation in terms of integral is given in [63, 66–68] as follows,

$$E_{\alpha}(z) = \frac{1}{2\pi} \int_C \frac{t^{\alpha-1} e^t}{t^{\alpha} - z} dt, \quad z \in \mathbb{C}, \quad Re(\alpha) > 0.$$

In this case, the path of integration C is a loop that encloses the disk's circles $|t| \leq |z|^{1/\alpha}$ in the positive sense: $|arg(t)| \leq \pi$ on C [63, 66–68]. It begins and ends at $-\infty$.

The two parameter Mittag-Leffler function's appropriate integral representation is provided by [63, 66–68] as follows:

$$E_{\alpha,\,\beta}(z) = \frac{1}{2\pi} \int_C \frac{t^{\alpha-\beta} e^t}{t^{\alpha} - z} dt, \quad z \in \mathbb{C}, \quad Re(\alpha) \text{ is } +ve.$$

Where C, the contour remains same as already defined above.

3. Modelling of the fractional diabetes mellitus system

The non-fractional model is given in [43] as below:

$$\begin{cases} \dfrac{dH}{dt} = -(\tau+\mu)H + \beta\theta + \sigma S, \\ \dfrac{dS}{dt} = -(\mu+\alpha_p+\beta(1-\theta)+\sigma)S + \tau H, \\ \dfrac{dD}{dt} = \omega T + \alpha_p S - (\lambda_p+\mu)D, \\ \dfrac{dC}{dt} = -(\mu+\delta+\gamma)C + \lambda_p D, \\ \dfrac{dT}{dt} = -(\mu+\omega)T + \gamma C, \end{cases}$$

such that the initial values at time $t = 0$ are given by H_0, S_0, D_0, C_0, and T_0. The state variables $H(t), S(t), D(t), C(t)$, and $T(t)$ represent totally healthy, suspected, confirmed without complications, confirmed with complications and confirmed with complications receiving treatment, respectively. The parameters γ, τ, θ, α_p, σ, ω, λ_p, μ, δ, and β, denote birth rate of children, healthy born children rate, naturally caused mortality rate, healthy population becoming suspected population rate, suspected population becoming healthy population rate, diabetes incidence rate probability, confirmed diabetic population developing complications rate, confirmed diabetic with complexity becoming without complexity rate, natural mortality with complexities rate and cured population rate from diabetes.

As an extension of the system above, the following diabetes mellitus mathematical system is considered using the fractional derivatives of order α. A system of linear differential equations with fractional order α is considered as:

$$\begin{cases} {}^cD_t^{\alpha} H = -(\tau+\mu)H + \beta\theta + \sigma S, \\ {}^cD_t^{\alpha} S = -(\mu+\alpha_p+\beta(1-\theta)+\sigma)S + \tau H, \\ {}^cD_t^{\alpha} D = \omega T + \alpha_p S - (\lambda_p+\mu)D, \\ {}^cD_t^{\alpha} C = -(\mu+\delta+\gamma)C + \lambda_p D, \\ {}^cD_t^{\alpha} T = -(\mu+\omega)T + \gamma C, \end{cases} \tag{9}$$

such that the initial values are same as stated above in the non-fractional model.

An autonomous vector field of a general form can be considered as below:

$$Y' = S(Y), \;\; Y \in R^n, \tag{10}$$

the corresponding fractional system after linearization can be defined as

$$^{c}D_{t}^{\alpha}\psi = J(E^{*})\psi,$$

such that the E^{*} represents the equilibrium points of the corresponding steady system given in 10, and $J(E^{*})$ represents Jacobian of the same system above. Negative real values are assumed from the Jacobian establishing the asymptotic stability of the system 10, as in [40].

4. Diabetes mellitus fractional system discretization by NSFDS

The fractional order diabetes mellitus system is discretized using the non-standard differences. On the basis of the guidelines in [16], the construction of the numerical scheme is carried out using non-standard differences. The development of the weight functions relies on the eigen-values of the matrix obtained from the fractional system.

• To counter the instabilities arising numerically, the discretized differential should be same as the differentials in the given system.

• A general form representing fractional discretized derivatives of order α is given below:

$$^{c}D_{t}^{\alpha}x \to \frac{x_{n+1} - \psi(h)x_{n}}{\phi(h)},$$

where $\psi(h,\ \alpha,\ p)$and $\phi(h,\ \alpha,\ p)$, where p is the set of model's parameters, are called the weight functions.

• Nonlocal terms are constructed in a discrete setting to replace the nonlinearities such that $s^{2} \to s_{n-1}^{2}$ and $s^{2} \to s_{n}s_{n-1}$.

• Furthermore, the corresponding difference model should be aligned with the original differential model in terms of the conditions imposed.

The positivity requirement from above is satisfied as the system is discretized in the following setup:

(i) For $H(t)$: $H(t) \to H(n+1)$ and $S(t) \to S(n)$ are used.

(ii) For $S(t)$ and $H(t)$: $H(t) \to H(n)$ and $S(t) \to S(n+1)$ are used.

(iii) For $S(t)$, $D(t)$, and $T(t)$: $S(t) \to S(n)$, $D(t) \to D(n+1)$, and $T(t) \to T(n)$ are used.

(iv) For $D(t)$ and $C(t)$: $D(t) \to D(n)$ and $C(t) \to C(n+1)$ are used.

(v) For $C(t)$ and $T(t)$: $C(t) \to C(n)$ and $T(t) \to T(n+1)$ are constructed.

Thus, the following discrete model is obtained:

$$\begin{cases} H(n+1) = \dfrac{H(n)+(\beta\theta+\sigma S(n))\phi_1}{1+(\mu+\tau)\phi_1}, \\ S(n+1) = \dfrac{S(n)+(\beta(1-\theta)+\tau H(n))\phi_2}{1+(\mu+\alpha_p+\sigma)\phi_2}, \\ D(n+1) = \dfrac{D(n)+(\alpha_p S(n)+\omega T(n))\phi_3}{1+(\mu+\lambda_p)\phi_3}, \\ C(n+1) = \dfrac{C(n)+\lambda_p\phi_4 D(n)}{1+(\mu+\delta+\gamma)\phi_4}, \\ T(n+1) = \dfrac{T(n)+\gamma\phi_5 C(n)}{1+(\mu+\omega)\phi_5}, \end{cases} \tag{11}$$

such that $\phi_i,\ i = 1 \to 5$ represents the corresponding weight functions to all the state variables given below as:

$$\begin{cases} \phi_1 = \dfrac{-E_\alpha(-(\mu+\tau)h)+1}{(\mu+\tau)}, \\ \phi_2 = \dfrac{-E_\alpha(-(\mu+\alpha_p+\sigma)h)+1}{(\mu+\alpha_p+\sigma)}, \\ \phi_3 = \dfrac{-E_\alpha(-(\mu+\lambda_p)h)+1}{(\mu+\lambda_p)}, \\ \phi_4 = \dfrac{-E_\alpha(-(\mu+\delta+\gamma)h)+1}{(\mu+\delta+\gamma)}, \\ \phi_5 = \dfrac{-E_\alpha(-(\mu+\omega)h)+1}{(\omega+\mu)}. \end{cases}$$

The standard finite differences carry the approximation errors over the iterations resulting in instabilities as numerical computations are performed. The above discretization using non-standard differences helps achieve better approximations as the construction and the consequent presence of the weight functions based on eigen-value decomposition incorporates better corrections as compared to the standard classical schemes such as Euler and Runge-Kutta discretizations.

4.1 *Analysis*

From the above model (9) we write in the matrix-vector formulation as follows:

$$(X^\alpha)' = AX + b, \tag{12}$$

where, $X^{\alpha} = [H^{\alpha},\ S^{\alpha},\ D^{\alpha},\ C^{\alpha},\ T^{\alpha}]^{T}$,

$$A = \begin{bmatrix} -(\tau+\mu) & \sigma & 0 & 0 & 0 \\ -(-\tau) & -(\alpha+\sigma+\mu) & 0 & 0 & 0 \\ 0 & \alpha & -(\lambda+\mu) & 0 & \omega \\ 0 & 0 & \lambda & -(\gamma+\delta+\mu) & 0 \\ 0 & 0 & 0 & \gamma & -(\omega+\mu) \end{bmatrix},$$

and

$$b = \begin{bmatrix} \beta\theta \\ \beta(1-\theta) \\ 0 \\ 0 \\ 0 \end{bmatrix}.$$

We decompose the matrix A such that equation (12) becomes

$$(X^{\alpha})' = P^{-1}DP + b. \tag{13}$$

Where D is the matrix of the eigen values and P is the matrix of the eigen vectors such that

$$P = [w_1,\ w_2,\ w_3,\ w_4,\ w_5].$$

We write the solution using the Mittag-Leffler function such that

$$U(t) = P \begin{bmatrix} c_1 E_{\alpha}(\lambda_1 t^{\alpha}) \\ c_2 E_{\alpha}(\lambda_2 t^{\alpha}) \\ c_3 E_{\alpha}(\lambda_3 t^{\alpha}) \\ c_4 E_{\alpha}(\lambda_4 t^{\alpha}) \\ c_5 E_{\alpha}(\lambda_5 t^{\alpha}) \end{bmatrix} + \begin{bmatrix} \beta\theta \\ \beta(1-\theta) \\ 0 \\ 0 \\ 0 \end{bmatrix},$$

or

$$U(t) = [w_1,\ w_2,\ w_3,\ w_4,\ w_5] \begin{bmatrix} c_1 E_{\alpha}(\lambda_1 t^{\alpha}) \\ c_2 E_{\alpha}(\lambda_2 t^{\alpha}) \\ c_3 E_{\alpha}(\lambda_3 t^{\alpha}) \\ c_4 E_{\alpha}(\lambda_4 t^{\alpha}) \\ c_5 E_{\alpha}(\lambda_5 t^{\alpha}) \end{bmatrix} + \begin{bmatrix} \beta\theta \\ \beta(1-\theta) \\ 0 \\ 0 \\ 0 \end{bmatrix},$$

where,

$$U(0) = [w_1,\ w_2,\ w_3,\ w_4,\ w_5] \begin{bmatrix} c_1 \\ c_2 \\ c_3 \\ c_4 \\ c_5 \end{bmatrix} + \begin{bmatrix} \beta\theta \\ \beta(-\theta+1) \\ 0 \\ 0 \\ 0 \end{bmatrix} = \begin{bmatrix} u_1(0) \\ u_2(0) \\ u_3(0) \\ u_4(0) \\ u_5(0) \end{bmatrix},$$

and

$$E_\alpha(\lambda t^\alpha) = \sum_{n=0}^{\infty} \frac{\lambda^\alpha (t)^{\alpha n}}{\Gamma(\alpha n+1)}.$$

5. Discretized fractional diabetes mellitus system stability

The stability of the discretized model is discussed in this section. The Lemma below outlines a special case when all the state variables, after incorporating the initial states, are all non-negative. We present the Lemma as:

Lemma 1 If the following inequality:

$$-((-\theta+1)\beta + \tau H(n)) \left\langle \frac{S(n)}{\phi_2} \right\rangle,$$

holds for $S,\ H,\ \beta,\ \theta,\ \tau$ and ϕ_2. Then all analytical representations of the state variables in (11) are positive along with the positive initial states.

The Lemma 1 has been proved in [43] by establishing the above inequality and the positive weight functions.

A local asymptotic stability result is presented below.

Theorem 5.1 [43] Suppose J is the Jacobian and E^* represents equilibrium points of the fractional system. Then the fractional system demonstrates asymptotic stability if real parts from $J(E^*)$ are all negative.

Proof. The equilibrium point of system 9 is obtained as $E^* = (H^*,\ S^*,\ D^*,\ C^*,\ T^*)$, where

$$H^* = \frac{\beta\theta}{\mu+\tau} + \left(\frac{\beta(1-\theta) + \dfrac{\beta\theta\tau}{\mu+\tau}}{(\mu+\alpha+\sigma) - \dfrac{\tau\sigma}{\mu+\tau}} \right) \frac{\sigma}{\mu+\tau},$$

$$S^* = \frac{\beta(1-\theta) + \dfrac{\beta\theta\tau}{\mu+\tau}}{(\mu+\alpha+\sigma) - \dfrac{\tau\sigma}{\mu+\tau}},$$

$$D^* = \frac{\alpha\beta(1-\theta)+\alpha\beta\theta\tau}{(\mu+\lambda)[(\mu+\alpha+\sigma)(\mu+\tau)-\tau\sigma]} + \frac{\left[\dfrac{\gamma\lambda\alpha\beta(1-\theta)-\dfrac{\gamma\lambda\alpha\beta\theta\tau}{\mu+\tau}}{-(\mu+\delta+\lambda)(\mu+\lambda)\left[(\mu+\alpha+\sigma)-\dfrac{\tau\sigma}{\mu+\tau}\right]}\right]}{-(\mu+\omega)+\dfrac{\gamma\lambda\omega}{(\mu+\lambda)(\mu+\delta+\gamma)}} \times \left[\frac{\omega}{\mu+\lambda}\right],$$

$$C^* = \frac{-\lambda\alpha\beta(1-\theta)+\dfrac{\lambda\alpha\beta\theta\tau}{\mu+\tau}}{-(\mu+\delta+\lambda)(\mu+\lambda)[(\mu+\alpha+\sigma)-\dfrac{\tau\sigma}{\mu+\tau}]}$$

$$+ \frac{\left[\dfrac{\gamma\lambda\alpha\beta(1-\theta)-\dfrac{\gamma\lambda\alpha\beta\theta\tau}{\mu+\tau}}{-(\mu+\delta+\lambda)(\mu+\lambda)\left[(\mu+\alpha+\sigma)-\dfrac{\tau\sigma}{\mu+\tau}\right]}\right]}{-(\mu+\omega)+\dfrac{\gamma\lambda\omega}{(\mu+\lambda)(\mu+\delta+\gamma)}} \times \left[\frac{\lambda\omega}{(\mu+\lambda)(\mu+\delta+\gamma)}\right],$$

$$T^* = \frac{\left[\dfrac{\gamma\lambda\alpha\beta(1-\theta)-\dfrac{\gamma\lambda\alpha\beta\theta\tau}{\mu+\tau}}{-(\mu+\delta+\lambda)(\mu+\lambda)\left[(\mu+\alpha+\sigma)-\dfrac{\tau\sigma}{\mu+\tau}\right]}\right]}{-(\mu+\omega)+\dfrac{\gamma\lambda\omega}{(\mu+\lambda)(\mu+\delta+\gamma)}}.$$

The Jacobian matrix of the continuous model at the equilibrium point $E^* = (H^*, S^*, D^*, C^*, T^*)$ determined as

$$J(H^*, S^*, D^*, C^*, T^*) = \begin{bmatrix} -(\mu+\tau) & \sigma & 0 & 0 & 0 \\ \tau & -(\mu+\alpha+\sigma) & 0 & 0 & 0 \\ 0 & \alpha & -(\mu+\lambda) & 0 & \omega \\ 0 & 0 & \lambda & -(\mu+\delta+\gamma) & 0 \\ 0 & 0 & 0 & \gamma & -(\mu+\omega) \end{bmatrix}.$$

Locally asymptotic stability of the fractional model can be analyzed by obtaining the eigenvalues of the Jacobian matrix at equilibrium points. Since all the eigen values of the Jacobian matrix are negative real numbers then the system is asymptotically stable.

We introduce the Schur-Cohn criterion for our system.

Lemma 2 [41] Consider the characteristic polynomial

$$q(\lambda) = \lambda^5 + a_1\lambda^4 + a_2\lambda^3 + a_3\lambda^2 + a_4\lambda + a_5,$$

where b_1, b_2, b_3, b_4, b_5 are constants. The zeros of the characteristic polynomial defined by above lie inside the unit disk if and only if the following conditions hold:

a. $q(1) > 0$,
b. $1 - b_1 + b_2 - b_3 + b_4 - b_5 > 0$,
c. The matrices

$$Q_4^{\pm} = \begin{bmatrix} 1 & 0 & 0 & 0 & 0 \\ b_1 & 1 & 0 & 0 & 0 \\ b_2 & b_1 & 1 & 0 & 0 \\ b_3 & b_2 & b_1 & 1 & 0 \\ b_4 & b_3 & b_2 & b_1 & 1 \end{bmatrix} \pm \begin{bmatrix} 0 & 0 & 0 & 0 & b_5 \\ 0 & 1 & 0 & b_5 & b_4 \\ 0 & 0 & b_5 & b_4 & b_3 \\ 0 & b_5 & b_4 & b_3 & b_2 \\ b_5 & b_4 & b_3 & b_2 & b_1 \end{bmatrix},$$

are positive.

Proof. One can conclude that if the Schur-Cohn criterion is satisfied, then the system is asymptotically stable. Therefore, the Jacobian matrix at the equilibrium point $E^* = (H^*, S^*, D^*, C^*, T^*)$ can be written as:

$$J^* = J(H^*, S^*, D^*, C^*, T^*) = \begin{bmatrix} h_1 & \phi_1\sigma h_1 & 0 & 0 & 0 \\ \phi_2\tau h_2 & h_2 & 0 & a_5 & b_4 \\ 0 & \phi_3\alpha h_3 & h_3 & 0 & \phi_3\omega h_3 \\ 0 & 0 & \phi_4\lambda h_4 & h_4 & 0 \\ 0 & 0 & 0 & \phi_5\gamma h_5 & h_5 \end{bmatrix},$$

where,

$$h_1 = \frac{1}{1 + \phi_1(\mu + \tau)},$$

$$h_2 = \frac{1}{1 + \phi_2(\mu + \alpha + \sigma)},$$

$$h_3 = \frac{1}{1 + \phi_3(\mu + \lambda)},$$

$$h_4 = \frac{1}{1 + \phi_4(\mu + \delta + \gamma)},$$

$$h_5 = \frac{1}{1 + \phi_5(\mu + \omega)},$$

where the coefficients are determined as

$$b_1 = -(h_1 + h_2 + h_3 + h_4 + h_5),$$

$$b_2 = (h_3 + h_4)h_5 + h_3h_4 + (h_1 + h_2)(h_3 + h_4 + h_5) - (1 - \tau\sigma\phi_1\phi_2)h_1h_2,$$

$$b_3 = -(1 + \gamma\lambda\omega\phi_3\phi_4\phi_5)h_3h_4h_5 + (\tau\sigma\phi_1\phi_2 - 1)h_1h_2(h_3 + h_4 + h_5) - (h_1 + h_2)[h_5(h_3 + h_4) + h_3h_4],$$

$$b_4 = (h_1 + h_2)(1 + \phi_3\phi_4\phi_5\lambda\omega\gamma) + h_1h_2(1 - \sigma\tau\phi_1\phi_2)[h_5(h_3 + h_4) + h_3h_4],$$

$$b_5 = h_1h_2h_3h_4h_5(\sigma\tau\phi_1\phi_2 - 1)(1 + \phi_3\phi_4\phi_5\lambda\omega\gamma),$$

we find the coefficients of the characteristic polynomial as below:

$$b_1 = -4.95460854,\ \ b_2 = 9.97630952,\ \ b_3 = -9.9657420912,\ \ b_4 = 4.9873210654,\ \ b_5 = -0.98322055324.$$

In the view of Lemma 2, since
a. $q(1) = 1 + b_1 + b_2 + b_3 + b_4 + b_5 = 0.213 \times 10^{-12} > 0$,
b. $-p(-1) = 1 - b_1 + b_2 - b_3 + b_4 - b_5 = 30.78648021 > 0$,
c. The matrices

$$Q_4^{\pm} = \begin{bmatrix} 1 & 0 & 0 & \pm b_5 \\ b_1 & 1 & \pm b_5 & \pm b_4 \\ b_2 & b_1 \pm b_5 & 1 \pm b_4 & \pm b_3 \\ b_3 \pm b_5 & b_2 \pm b_4 & b_1 \pm b_3 & 1 \pm b_2 \end{bmatrix}.$$

As all the axioms of Schur-Cohn are established, the given system is asymptotically stable locally for the chosen parameters.

6. Numerical experiment

This section represents numerical experiment in order to make analytical results, standard finite differences and the non-standard finite difference approximations. The parameter values are chosen such that $\theta = 0.913,\ \beta = 0.037,\ \tau = 0.035,\ \mu = 0.51,\ \sigma = 0.081,\ \lambda_p = 0.512,\ \alpha_p = 0.0231,\ \delta = 0.02001,\ \omega = 0.079,$ and $\gamma_p = 0.081$. The eigen values are calculated using the matrix A given in (12).

$$\begin{pmatrix} \lambda_1 \\ \lambda_2 \\ \lambda_3 \\ \lambda_4 \\ \lambda_5 \end{pmatrix} = \begin{pmatrix} -0.596819223081673 \\ -0.310501484379986 \\ -0.252031242374329 \\ -0.123968757625671 \\ -0.126679292538342 \end{pmatrix}.$$

Since all the eigen values are negative real numbers, Theorem 5.1 dictates the asymptotic stability of the fractional system locally. The corresponding eigen vectors are given as follows:

$$w_1 = \begin{pmatrix} 5.896221210428095 \times 10^{-17} \\ 1.650399374969535 \times 10^{-16} \\ -0.596315604210655 \\ 0.7870714682318165 \\ -0.1578803473213 \end{pmatrix}, \quad w_2 = \begin{pmatrix} 7.085776189609232 \times 10^{-16} \\ -7.225923671895149 \times 10^{-16} \\ 0.1490848796756575 \\ -0.8058512826844632 \\ 0.5730422400206641 \end{pmatrix},$$

$$w_3 = \begin{pmatrix} 0.6221573520391458 \\ -0.7312778595570425 \\ 0.01064184857958888 \\ -0.1563541004840987 \\ 0.2315017661831681 \end{pmatrix}, \quad w_4 = \begin{pmatrix} -0.44704799767537 \\ -0.1901699845231093 \\ -0.1107453024216173 \\ -0.5888750357075574 \\ -0.6363529956501267 \end{pmatrix}, \quad w_5 = \begin{pmatrix} -1.085147452761105 \times 10^{-15} \\ -4.908431230456085 \times 10^{-16} \\ 0.120651887117552 \\ 0.6605943518791119 \\ 0.7409846316897467 \end{pmatrix}.$$

The comparison of the FDS and the NSFDS using time series solutions for the state variables $H(t)$ (healthy individuals), $S(t)$ (susceptible individuals), $D(t)$ (diabetic without complications individuals), $C(t)$ (Diabetic with comlications individuals , and $T(t)$ Diabetic with com lications receivin a cure individuals in figure 1). These solutions are compared using the analytical solution (green solid line), the standard finite difference scheme (FDS, blue dashed line), and the non-standard finite difference scheme (NSFDS, red dashed line with arrows).

For $H(t)$, the FDS differs from the analytical solution significantly after $t = 2$, while the NSFDS stays close to the analytical solution. Similarly, for $S(t)$, the FD method shows more prominent deviations after $t = 4$, whereas the NSFDS remains closer to the analytical solution throughout the time domain. In the case of $D(t)$, the FDS shows considerable differences in the decreasing phase after $t = 2$, while the NSFDS method accurately follows both the peak and the subsequent decrease. For $C(t)$, the FDS outgrows significantly during the decreasing phase after $t = 3$, whereas the NSFDS shows a closer agreement with the analytical solution. Finally, for $T(t)$, the FDS strays more as time progresses, particularly after $t = 4$, while the NSFDS remains close to the analytical solution throughout. Overall, the NSFDS method consistently follows the analytical solution more closely across all state variables, exhibiting better accuracy and stability, whereas the FD method exhibits larger differences, particularly as time progresses, indicating less accurate approximation.

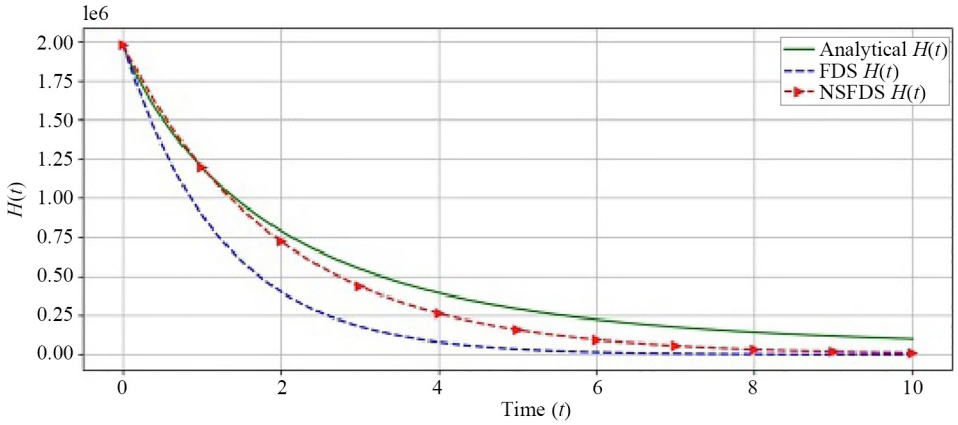

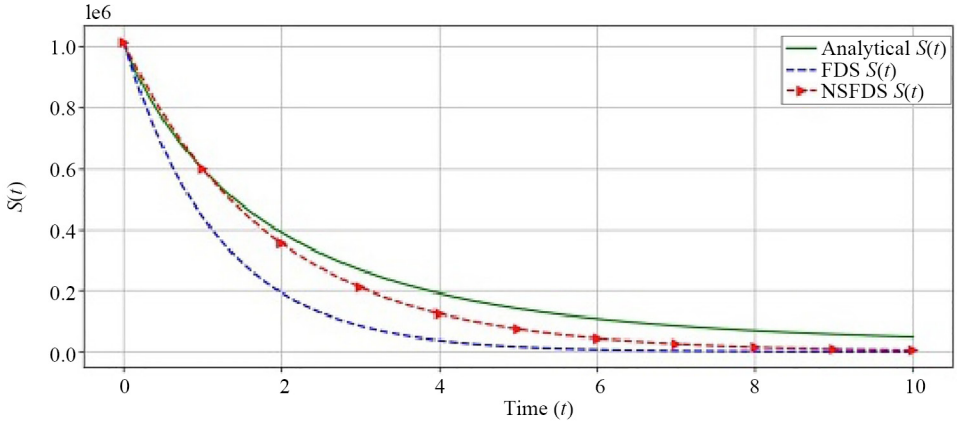
1e6
1.0
0.8
0.6
0.4
0.2
0.0
S(t)
0
2
4
6
8
10
Time (t)
Analytical S(t)
FDS S(t)
NSFDS S(t)

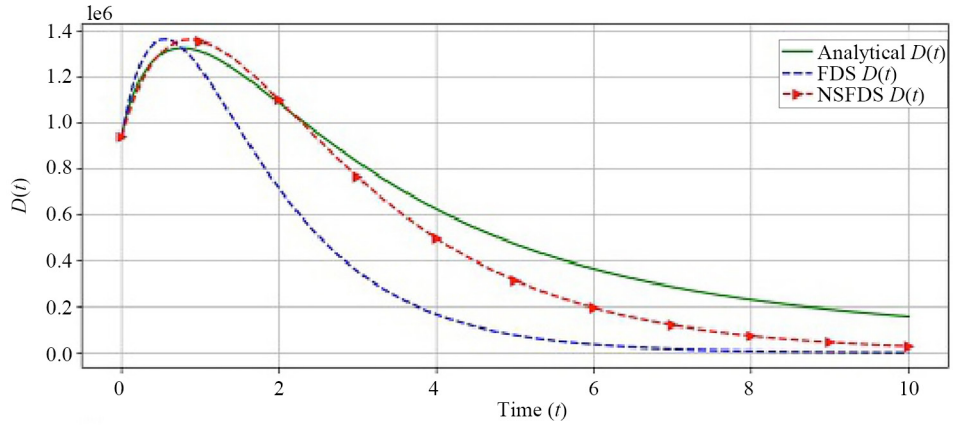
1e6
1.4
1.2
1.0
0.8
0.6
0.4
0.2
0.0
D(t)
0
2
4
6
8
10
Time (t)
Analytical D(t)
FDS D(t)
NSFDS D(t)

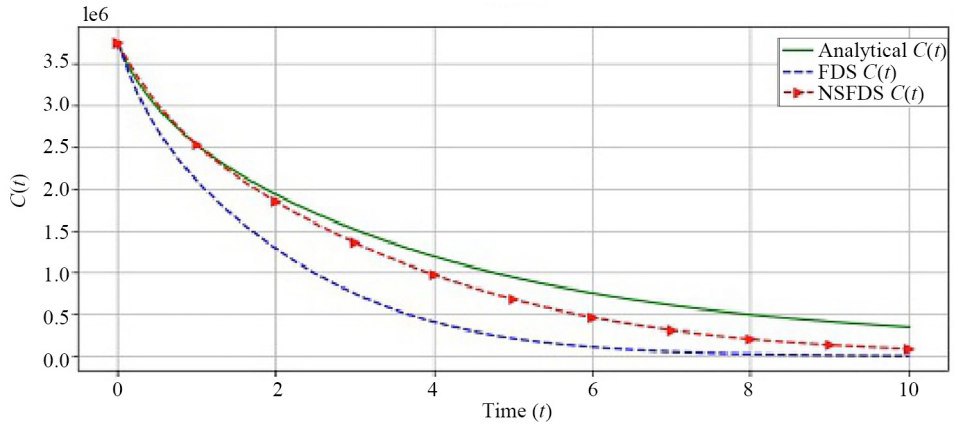
1e6
3.5
3.0
2.5
2.0
1.5
1.0
0.5
0.0
C(t)
0
2
4
6
8
10
Time (t)
Analytical C(t)
FDS C(t)
NSFDS C(t)

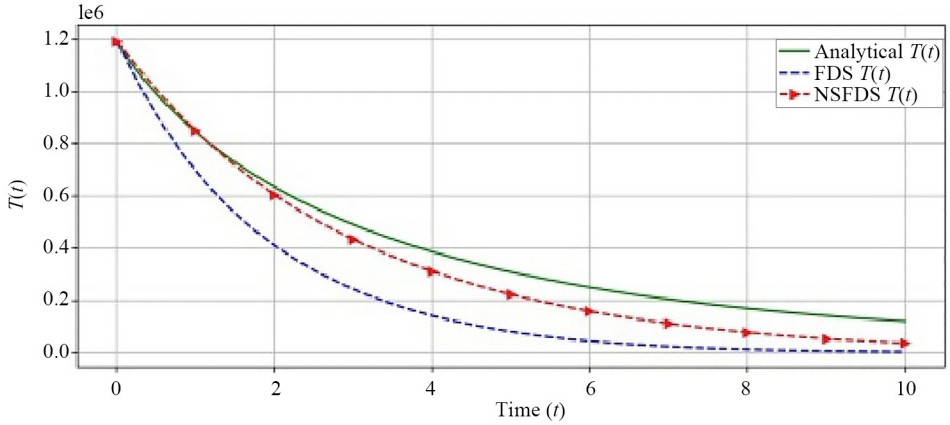

Figure 1. Comparison between FDS and NSFDS using time series for $\theta = 0.913$, $\beta = 0.037$, $\tau = 0.035$, $\mu = 0.51$, $\sigma = 0.081$, $\lambda_p = 0.512$, $\alpha_p = 0.0231$, $\delta = 0.02001$, $\omega = 0.079$, and $\gamma_p = 0.081$

6.1 *Error magnitude*

In this section, the error between the FDS and the NSFDS is compared by using the heat maps. Both the schemes, side by side for each state variable are compared. Each heat map illustrates the error magnitude over time for the approximations. The time range is from 0 to 10, with the y-axis labeled "Index" representing the different time steps within this interval. The error magnitude is depicted using a color scale, ranging from 10^{-10} to 10^{-2}. The left panels in all the figures (Figure 2 to Figure 6) compare the error between the FDS and the analytical solution, the right panels compare the NSFDS and the analytical solution.

In the FDS heat map (left), the error is uniformly represented in a green hue across all time steps, indicating a consistent error magnitude closer to 10^{-4} throughout the entire time interval. This suggests that the FDS maintains a relatively stable error but at a higher magnitude compared to the NSFDS. The NSFDS heat map (right) shows a predominantly blue to purple color, corresponding to lower error magnitudes closer to 10^{-8} to 10^{-10} for most time steps. This shows that the FDS maintains a uniform but higher error throughout the simulation, the NSFDS achieves significantly lower errors.

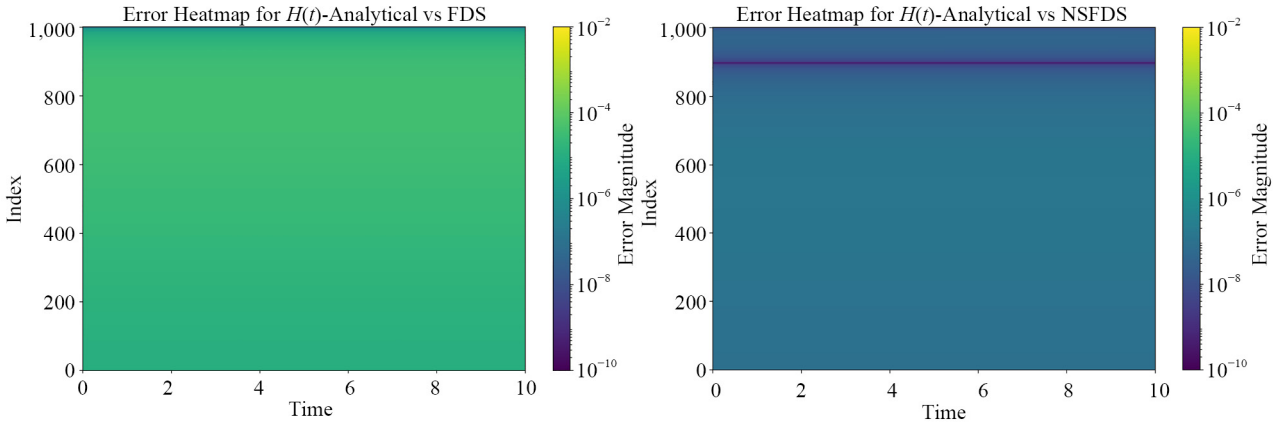

Figure 2. Heatmap for $H(t)$ for error comparison between FDS and NSFDS

In the case of $S(t)$, the FDS (left panel) exhibits errors up to 10^{-4}, uniformly distributed across the time steps, indicating a consistent error magnitude throughout the simulation. On the other hand, the NSFDS (right panel) demonstrates significantly lower errors, ranging between 10^{-6} and 10^{-8}. This suggests that while the FDS maintains a steady but higher error, the NSFDS performs more accurately across most of the time interval.

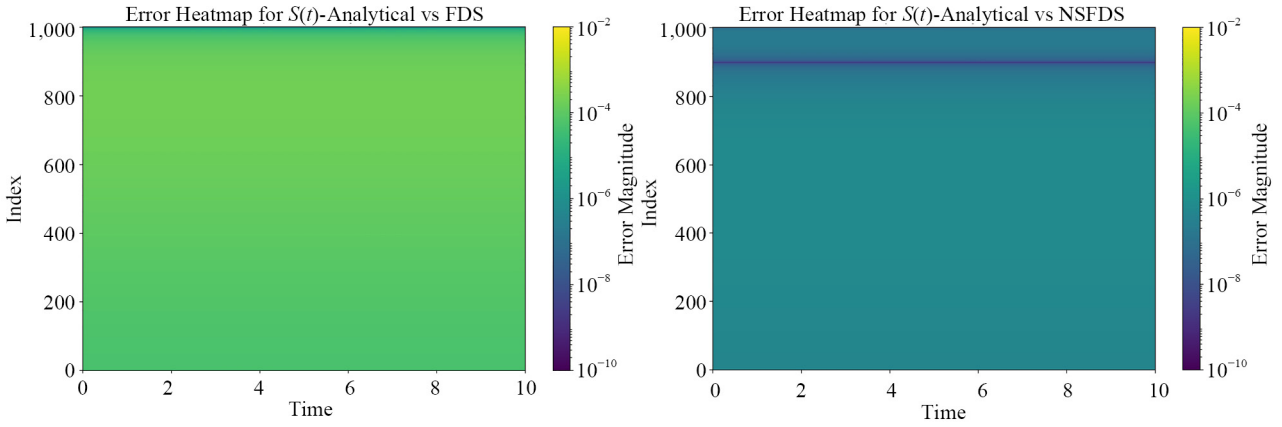

Figure 3. Heatmap for $S(t)$ for error comparison between FDS and NSFDS

In the case of $D(t)$, the error heat maps present a smooth pattern. For the FDS (left panel), the error remains relatively constant throughout the majority of the simulation time but shows an increase towards the upper values (closer to the end of the time interval). The error magnitude is around 10^{-4} with a slight increase to 10^{-2} near the end. On the other hand, the NSFDS (right panel) shows a more stable pattern where the error is much less, with values around 10^{-7} to 10^{-6}. This further establishes the better accuracy of the NSFDS in approximating the analytical solution for $D(t)$.

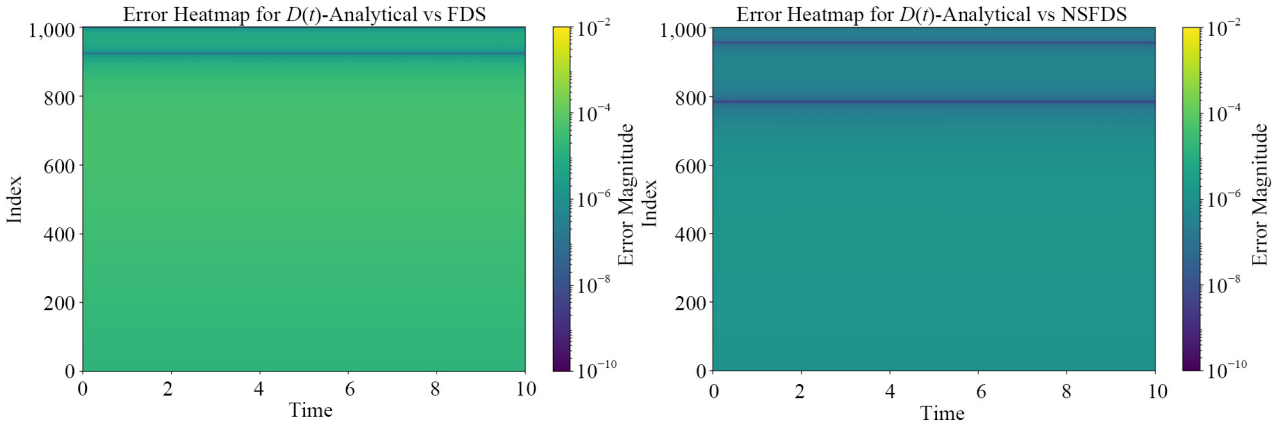

Figure 4. Heatmap for $D(t)$ for error comparison between FDS and NSFDS

In the case of $C(t)$, the FDS (left panel) shows a uniform error distribution, with the magnitude of the error generally ranging from 10^{-5} to 10^{-4}, and highest around 10^{-2}. The uniform green-yellow color suggests that the error remains fairly same throughout the simulation period, with some higher error accumulation towards the upper values for the later time steps. Oppositely, the NSFDS (right panel) displays a significantly better performance, with errors hovering around 10^{-8} to 10^{-6}.

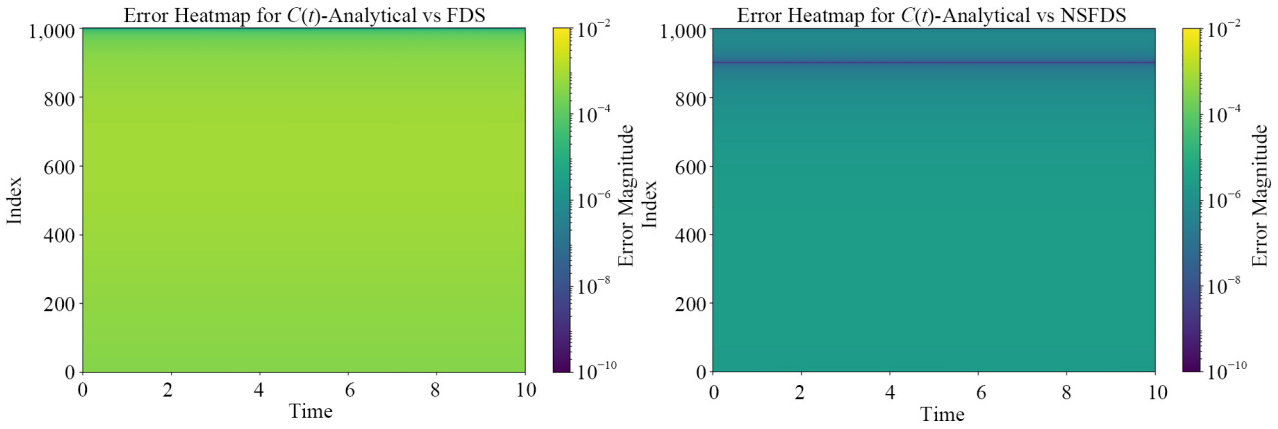

Figure 5. Heat map for $C(t)$ for error comparison between FDS and NSFDS

Lastly, in the case of $T(t)$, the FDS (left panel) shows a relatively uniform error magnitudes, ranging from 10^{-5} to 10^{-3}, such that the highest value is at 10^{-2}. This is represented by the green to yellow filling, indicating a moderate error level throughout the time steps. On the other hand, the NSFDS (right panel) demonstrates significantly better performance, with errors predominantly within the range of 10^{-8} to 10^{-6}.

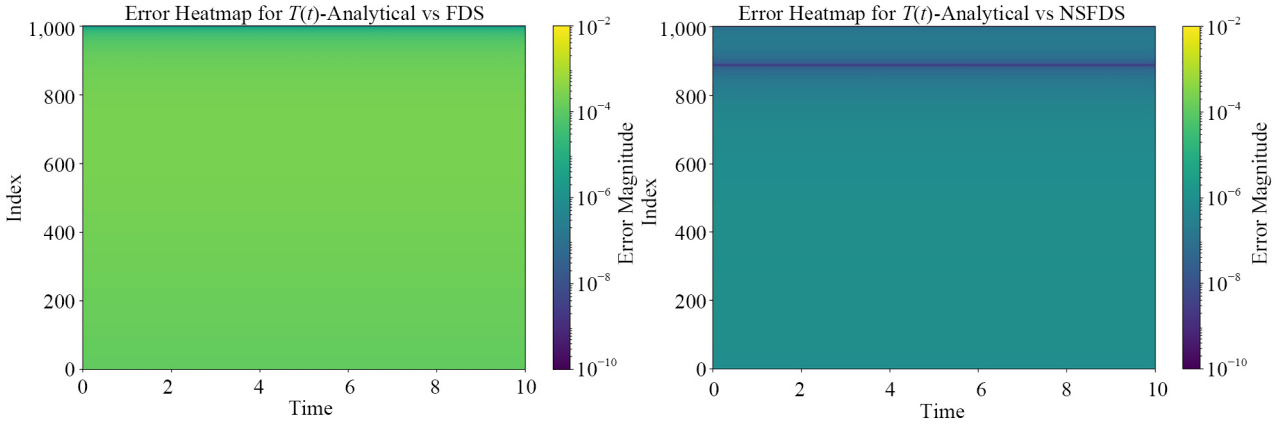

Figure 6. Heat map for $T(t)$ for error comparison between FDS and NSFDS

Across all state variables, the NSFDS demonstrates consistently lower error magnitudes compared to the standard FDS. This suggests that the NSFDS offers a more accurate and reliable approximation of the analytical solution over the given time period.

6.2 *Convergence rate analysis*

In figures 7-11, the convergence rate analysis based on the step sizes and the magnitude of the error for all the state variables are discussed. The convergence rate plots display the error magnitudes for the state variable approximations using both the FDS and NSFDS for step sizes $h = 10^{-3}$, 10^{-2}, and 10^{-1}.

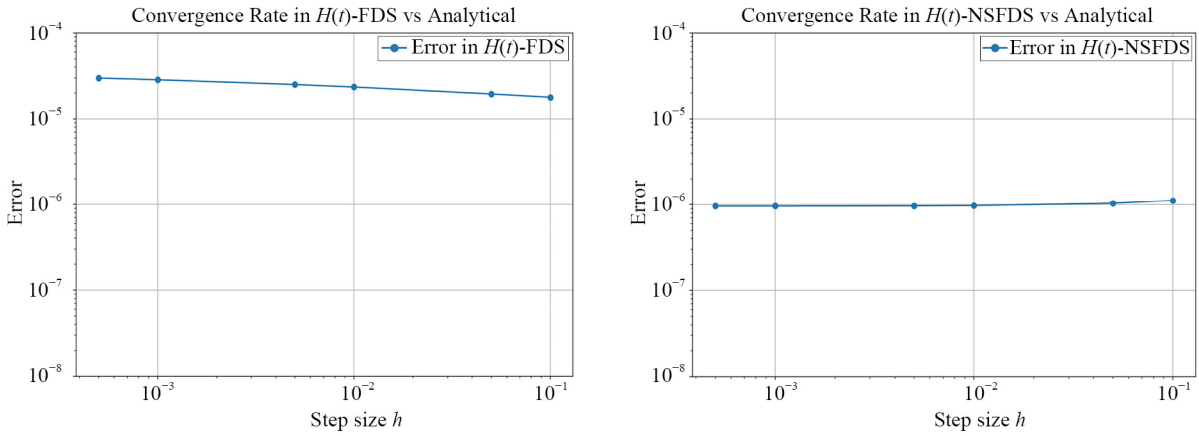

Figure 7. Convergence rate of $H(t)$ for error comparison between FDS and NSFDS at different step sizes

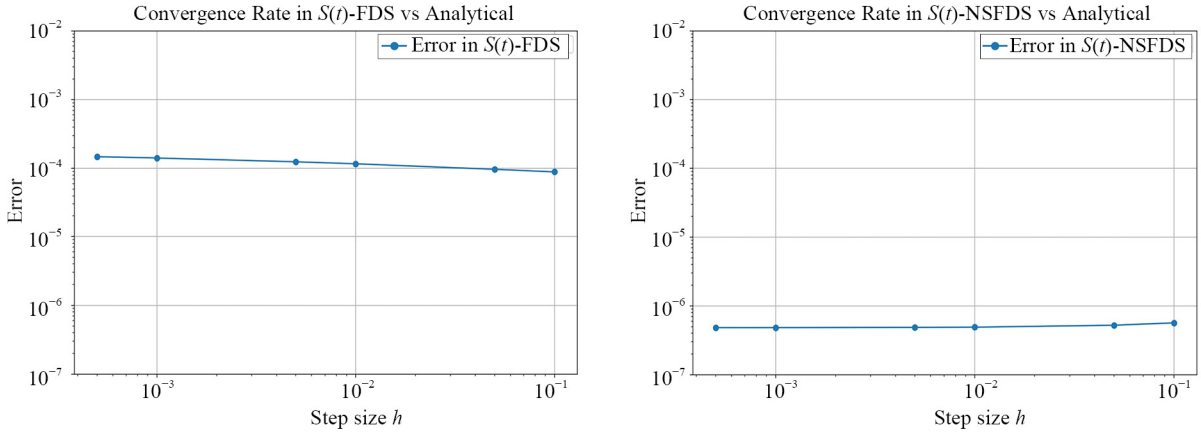

Figure 8. Convergence rate of $S(t)$ for error comparison between FDS and NSFDS at different step sizes

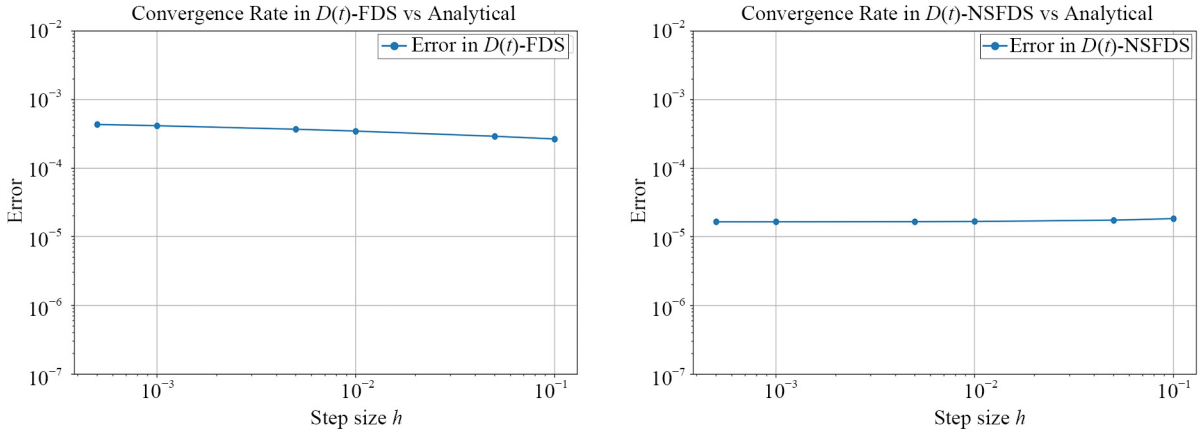

Figure 9. Convergence rate of $D(t)$ for error comparison between FDS and NSFDS at different step sizes

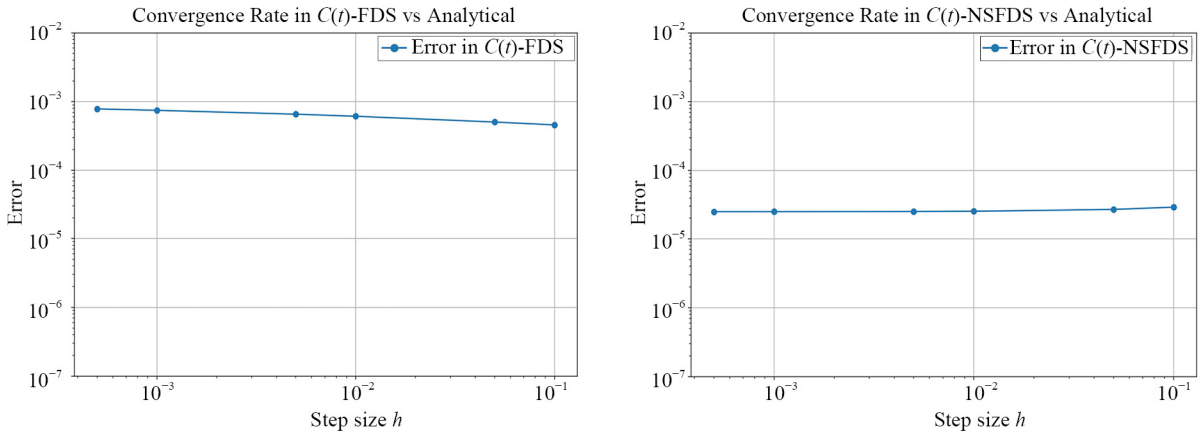

Figure 10. Convergence rate of $C(t)$ for error comparison between FDS and NSFDS at different step sizes

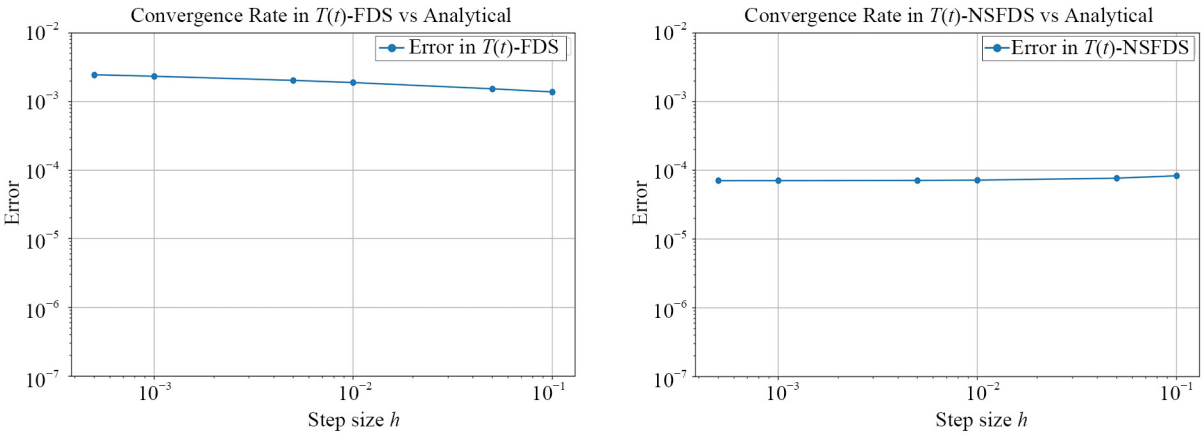

Figure 11. Convergence rate of $T(t)$ for error comparison between FDS and NSFDS at different step sizes

The analysis of the convergence rates reveals a uniform pattern when comparing the FDS with the NSFDS. For $H(t)$, the FDS starts with an error of approximately 10^{-4} at the smallest step size $h = 10^{-3}$ and slowly decreases to about 6×10^{-5} as the step size increases to $h = 10^{-1}$. On the other hand, the NSFDS demonstrates a superior performance by maintaining a much lower and stable error around 10^{-6} throughout all step sizes. A similar behaviour is observed for $S(t)$, where the FDS shows a stepwise reduction in error from approximately 10^{-4} at $h = 10^{-3}$ to 4×10^{-5} at $h = 10^{-1}$, while the NSFDS uniformly holds the error around 10^{-6}, signifying its accuracy. For $D(t)$ and $C(t)$, the FDS begins with an error close to 10^{-3} and reduces to around 10^{-4} as the step size increases, but it still remains considerably higher compared to the NSFDS, which maintains an error level at approximately 10^{-5} across all step sizes. This uniform low error indicates the NSFDS's ability to closely follow the analytical solution, regardless of the step size. Lastly, for $T(t)$, the FDS shows a similar error reduction behaviour from 10^{-2} to 10^{-3} as the step size increases, while the NSFDS maintains an even more stable error close to 10^{-5} across all tested step sizes. This detailed analysis shows the NSFDS's better accuracy and stability, making it a more reliable computational technique for accurately solving the fractional diabetes mellitus system of differential equations with varying step sizes. Overall, the NSFDS exhibits a significantly lower and more stable error magnitude across all state variables and step sizes.

7. Conclusion

This paper applies the NSFDS to numerically solve the system of linear fractional differential equations that model diabetes mellitus. This scheme is found to be stable and more accurate than the FDS up to step size $h = 10^{-3}$. The comparison of the FDS and the NSFDS using time series solutions for the state variables $H(t)$ (healthy individuals), $S(t)$ (susceptible individuals), $D(t)$ (diabetic without complications individuals), $C(t)$ (Diabetic with complications individuals) and $T(t)$ (Diabetic with complications receiving a cure individuals) are presented. These solutions are compared using the analytical solution (green solid line), the standard finite difference scheme (FDS, blue dashed line) and NSFDS, red dashed line with arrows. The NSFDS method consistently follows the analytical solution more closely across all state variables, indicating better accuracy and stability, whereas the FDS exhibits larger differences, particularly as time progresses, indicating less accurate approximation. This demonstrates the better performance of the NSFDS method in approximating the analytical solution of the fractional diabetic model. The heat maps compare the errors between the analytical solution and two numerical methods: the standard finite difference FDS and the NSFDS. Each heat map illustrates the error magnitude over time for the state variables. Across all state variables, the NSFDS demonstrates consistently lower error magnitudes compared to the standard FDS. This suggests that the NSFDS offers a more accurate and reliable approximation of the analytical solution over the given time period. The heat maps effectively visualize these differences, with the NSFDS providing better performance in reducing errors for the fractional diabetic model. The convergence rate analysis discussed here, is based on the step sizes and the magnitude of the error for all the state variables. The convergence rate plots display the error magnitudes using both the FDS and NSFDS for step sizes $h = 10^{-3}$, 10^{-2}, and 10^{-1}.

Acknowledgement

We are thankful to the reviewers for their valuable suggestions.

Confilict of interest

The authors declare no competing financial interest.

References

[1] Boutayeb A, Twizell EH, Achouayb K, Chetouani A. A mathematical model for the burden of diabetes and its complications. *Biomedical Engineering Online*. 2004; 3(1): 1-8.

[2] Akinsola VO, Oluyo TO. Analytic solution of mathematical model of the complications and control of diabetes mellitus using fundamental matrix method. *Journal of Interdisciplinary Mathematics*. 2020; 23(4): 877-884.

[3] Akinsola VO, Oluyo TO. A Note on the divergence of the numerical solution of the mathematical model for the burden of diabetes and its complications using euler method. *International Journal of Mathematics and Computer Applications Research*. 2015; 5(3): 93-100.

[4] Akinsola VO, Oluyo TO. Mathematical analysis with numerical solutions of the mathematical model for the complications and control of diabetes mellitus. *Journal of Statistics and Management Systems*. 2019; 22(5): 845-869.

[5] AlShurbaji M, Kader LA, Hannan H, Mortula M, Husseini GA. Comprehensive study of a diabetes mellitus mathematical model using numerical methods with stability and parametric analysis. *International Journal of Environmental Research and Public Health*. 2023; 20(2): 939.

[6] Vanitha R, Porchelvi R. A linear population model for diabetes mellitus. *Bulletin of Pure and Applied Sciences-Mathematics and Statistics*. 2017; 36(2): 311-315.

[7] Boutayeb A, Chetouani A, Achouyab A, Twizell EH. A non-linear population model of diabetes mellitus. *Journal of Applied Mathematics and Computing*. 2006; 21(1): 127-139.

[8] de Oliveira SR, Raha S, Pal D. Global asymptotic stability of a non-linear population model of diabetes mellitus. In: *Differential and Difference Equations with Applications: ICDDEA, Amadora, Portugal, May 2015, Selected Contributions*. Heidelberg: Springer International Publishing; 2016. p.351-357.

[9] Boutayeb W, Lamlili ME, Boutayeb A, Derouich M. The dynamics of a population of healthy people, pre-diabetics and diabetics with and without complications with optimal control. In: *Proceedings of the Mediterranean Conference on Information & Communication Technologies 2015*. Heidelberg: Springer International Publishing; 2016. p.463-471.

[10] Permatasari AH, Tjahjana RH, Udjiani T. Global stability for linear system and controllability for nonlinear system in the dynamics model of diabetics population. *Journal of Physics Conference Series*. 2018; 1025(1): 012086.

[11] Widyaningsih P, Affan RC, Saputro DR. A mathematical model for the epidemiology of diabetes mellitus with lifestyle and genetic factors. *Journal of Physics Conference Series*. 2018; 1028: 012110. Available from: https://doi.org/:10.1088/1742-6596/1028/1/012110.

[12] Aye PO. Stability analysis of mathematical model for the dynamics of diabetes mellitus and its complications in a population. *Data Analytics and Applied Mathematics*. 2022; 3(1): 20-27.

[13] Aye PO. Analysis of mathematical model for the dynamics of diabetes mellitus and its complications. *Applied Mathematics and Computational Intelligence*. 2021; 10(2021): 57-77.

[14] Aye PO. Mathematical analysis of the effect of control on the dynamics of diabetes mellitus and its complications. *Earthline Journal of Mathematical Sciences*. 2021; 6(2): 375-395.

[15] Miekens RE. *Difference Equations: Theory and Applications*. USA: Chapman and Hall/CRC; 1990.

[16] Mickens RE. *Advances in the Applications of Nonstandard Finite Diffference Schemes*. Singapore: World Scientific Publishing; 2005.

[17] Mickens RE. *Nonstandard Finite Difference Models of Differential Equations*. Singapore: World Scientific Publishing; 1993.

[18] Mickens RE. Nonstandard finite difference schemes for differential equations. *Journal of Difference Equations and Applications*. 2002; 8(9): 823-847.

[19] Mickens RE. Calculation of denominator functions for nonstandard finite difference schemes for differential equations satisfying a positivity condition. *Numerical Methods for Partial Differential Equations: An International Journal*. 2007; 23(3): 672-691.

[20] Mickens RE. Exact solutions to a finite-difference model of a nonlinear reaction-advection equation: Implications for numerical analysis. *Numerical Methods for Partial Differential Equations*. 1989; 5(4): 313-325.

[21] Patidar KC. On the use of nonstandard finite difference methods. *Journal of Difference Equations and Applications*. 2005; 11(8): 735-758.

[22] Patidar KC. Nonstandard finite difference methods: Recent trends and further developments. *Journal of Difference Equations and Applications*. 2016; 22(6): 817-849.

[23] Adekanye O, Washington T. Nonstandard finite difference scheme for a tacoma narrows bridge model. *Applied Mathematical Modelling*. 2018; 62: 223-236. Available from: https://doi.org/10.1016/j.apm.2018.05.027.

[24] Anguelov R, Berge T, Chapwanya M, Djoko JK, Kama P, Lubuma JS, et al. Nonstandard finite difference method revisited and application to the Ebola virus disease transmission dynamics. *Journal of Difference Equations and Applications*. 2020; 26(6): 818-854.

[25] Arenas AJ, Gonzalez-Parra G, Chen-Charpentier BM. Construction of nonstandard finite difference schemes for the SI and SIR epidemic models of fractional order. *Mathematics and Computers in Simulation*. 2016; 121: 48-63. Available from: https://doi.org/10.1016/j.matcom.2015.09.001.

[26] Baleanu D, Zibaei S, Namjoo M, Jajarmi A. A nonstandard finite difference scheme for the modeling and nonidentical synchronization of a novel fractional chaotic system. *Advances in Difference Equations*. 2021; 2021(1): 308.

[27] Dang QA, Hoang MT. Lyapunov direct method for investigating stability of nonstandard finite difference schemes for metapopulation models. *Journal of Difference Equations and Applications*. 2018; 24(1): 15-47.

[28] Kocabıyık M, Özdoğan N, Ongun MY. Nonstandard finite difference scheme for a computer virus model. *Journal of Innovative Science and Engineering*. 2020; 4(2): 96-108.

[29] Dang QA, Hoang MT. Numerical dynamics of nonstandard finite difference schemes for a computer virus propagation model. *International Journal of Dynamics and Control*. 2020; 8(3): 772-778.

[30] Özdoğan N, Ongun MY. Dynamical behaviours of a discretized model with michaelis-menten harvesting rate. *Journal of Universal Mathematics*. 2022; 5(2): 159-176.

[31] Kocabiyik M, Ongun MY. Construction a distributed order smoking model and its nonstandard finite difference discretization. *AIMS Mathematics*. 2021; 7(3): 4636-4654.
[32] Yakit Ongun M, Arslan D. Explicit and implicit schemes for fractional-order hantavirus model. *Iranian Journal of Numerical Analysis and Optimization*. 2018; 8(2): 75-94.
[33] Shabbir MS, Din Q, Safeer M, Khan MA, Ahmad K. A dynamically consistent nonstandard finite difference scheme for a predator-prey model. *Advances in Difference Equations*. 2019; 2019(1): 1-17.
[34] Vaz S, Torres DF. A dynamically-consistent nonstandard finite difference scheme for the SICA model. *Mathematical Biosciences and Engineering*. 2021; 18(4): 4552-4571.
[35] Egbelowo O, Harley C, Jacobs B. Nonstandard finite difference method applied to a linear pharmacokinetics model. *Bioengineering*. 2017; 4(2): 40.
[36] Khan IU, Mustafa S, Shokri A, Li S, Akgül A, Bariq A. The stability analysis of a nonlinear mathematical model for typhoid fever disease. *Scientific Reports*. 2023; 13(1): 15284.
[37] Özköse F, Yavuz M. Investigation of interactions between COVID-19 and diabetes with hereditary traits using real data: A case study in Turkey. *Computers in Biology and Medicine*. 2022; 141: 105044.
[38] Atangana A, Araz Sİ. Mathematical model of COVID-19 spread in Turkey and South Africa: Theory, methods, and applications. *Advances in Difference Equations*. 2020; 2020(1): 659.
[39] Gümüs ÖA, Cui Q, Selvam GM, Vianny A. Global stability and bifurcation analysis of a discrete time SIR epidemic model. *Miskolc Mathematical Notes*. 2022; 23(1): 193-210.
[40] Wiggins S. *Introduction to Applied Nonlinear Dynamical Systems and Chaos*. New York: Springer; 2003.
[41] Elaydi SN, Elaydi SN. Oscillation theory. In: *An Introduction to Difference Equations*. New York: Springer; 1999. p.296-314.
[42] Kathiri SA, Bashier EBM, Hamid NNA, Ramli N. Development of a non-standard finite difference method for solving a fractional decay model. *Journal of Applied Mathematics and Informatics*. 2024; 42(3): 695-708.
[43] Çetinkaya İT. An application of nonstandard finite difference method to a model describing diabetes mellitus and its complications. *Journal of New Theory*. 2023; 2023(45): 105-119.
[44] Miller KS. *An Introduction to the Fractional Calculus and Fractional Differential Equations*. USA: John Willey Aand Sons; 1993.
[45] Das S. *Functional Fractional Calculus*. Berlin: Springer; 2011.
[46] Podlubny I. *Fractional Differential Equations, Mathematics in Science and Engineering, vol. 198*. San Diego: Academic Press; 1999.
[47] Diethelm K, Ford NJ. Analysis of fractional differential equations. *Journal of Mathematical Analysis and Applications*. 2002; 265(2): 229-248.
[48] Kilbas AAA, Srivastava HM, Trujillo JJ. *Theory and Applications of Fractional Differential Equations*. Amsterdam, Netherlands: Elsevier; 2006.
[49] Caputo M. Linear models of dissipation whose *Q* is almost frequency independent-II. *Geophysical Journal International*. 1967; 13(5): 529-539.
[50] Jumarie G. Modified riemann-liouville derivative and fractional taylor series of nondifferentiable functions further results. *Computers and Mathematics with Applications*. 2006; 51(9-10): 1367-1376.
[51] Ghosh U, Sengupta S, Sarkar S, Das S. Characterization of non-differentiable points in a function by fractional derivative of Jumarrie type. *European Journal of Academic Essays*. 2015; 2(2): 70-86.
[52] Diethelm K, Ford NJ, Freed AD. A predictor-corrector approach for the numerical solution of fractional differential equations. *Nonlinear Dynamics*. 2002; 29(1-4): 3-22.
[53] Hu Y, Luo Y, Lu Z. Analytical solution of the linear fractional differential equation by Adomian decomposition method. *Journal of Computational and Applied Mathematics*. 2008; 215(1): 220-229.
[54] Ray SS, Bera RK. An approximate solution of a nonlinear fractional differential equation by adomian decomposition method. *Applied Mathematics and Computation*. 2005; 167(1): 561-571.
[55] Abdulaziz O, Hashim I, Momani S. Application of homotopy-perturbation method to fractional IVPs. *Journal of Computational and Applied Mathematics*. 2008; 216(2): 574-584.
[56] Molliq RY, Noorani MS, Hashim I, Ahmad RR. Approximate solutions of fractional Zakharov-Kuznetsov equations by VIM. *Journal of Computational and Applied Mathematics*. 2009; 233(2): 103-108.
[57] Ertürk VS, Momani S. Solving systems of fractional differential equations using differential transform method. *Journal of Computational and Applied Mathematics*. 2008; 215(1): 142-151.

[58] Ghosh U, Sengupta S, Sarkar S, Das S. Analytic solution of linear fractional differential equation with Jumarie derivative in term of Mittag-Leffler function. *American Journal of Mathematical Analysis*. 2015; 3(2): 32-38.
[59] Alzaid SS, Shaw PK, Kumar S. A numerical study of fractional population growth and nuclear decay model. *AIMS Mathematics*. 2022; 7(6): 11417-11442.
[60] Alqhtani M, Saad KM. Numerical solutions of space-fractional diffusion equations via the exponential decay kernel. *AIMS Mathematics*. 2022; 7(4): 6535-6549.
[61] Mickens RE. *Advances in the Applications of Nonstandard Finite Diffference Schemes*. Singapore: World Scientific Publishing; 2005.
[62] Bashier EB. *Practical Numerical and Scientific Computing with MATLAB® and Python*. USA: CRC Press; 2020.
[63] Mittag-Leffler GM. Sur la nouvelle fonction $E_a(x)$. *Comptes Rendus de l'Académie des Sciences, Paris*. 1903; 137(2): 554-558.
[64] Wiman A. Über den fundamentalsatz in der teorie der funktionen $E_a(x)$. *Acta Mathematica*. 1905; 29: 191-201, 1905. Available from: https://doi.org/10.1007/BF02403202.
[65] Prabhakar TR. A singular integral equation with a generalized mittag leffler function in the kernel. *Yokohama Mathematical Journal*. 1971; 19(1): 7-15.
[66] Erdelyi A. *Asymptotic Expansions*. USA: Dover Publications, Inc; 1956.
[67] Erdelyi A. *Tables of Integral Transforms, vol. 1*. USA: McGraw-Hill Education; 1954.
[68] Erdelyi A. *On Some Functional Transformation*. Italy: Politecnico di Torino; 1950.